

Enhancing Porous Alumina Ceramics for Bioapplications Through Targeted Surface Modification Techniques



Sarah Shafi Kizar*^{ORCID}, Israa K. Sabree^{ORCID}

Ceramic and Building Materials Engineering Department, Faculty of Materials Engineering, University of Babylon, Babylon 51001, Iraq

Corresponding Author Email: stud70098@gmail.com

Copyright: ©2024 The authors. This article is published by IETA and is licensed under the CC BY 4.0 license (<http://creativecommons.org/licenses/by/4.0/>).

<https://doi.org/10.18280/acsm.480212>

ABSTRACT

Received: 9 February 2024

Revised: 4 April 2024

Accepted: 16 April 2024

Available online: 30 April 2024

Keywords:

inert ceramic porous alumina, alkaline treatment, amino acid treatment, UV treatment

Porous bioceramics are commonly used as support structures for bone growth and repair. However, their mechanical properties have been limited by high macroporosity and microporosity. Alumina ceramics (Al_2O_3) are preferred for bone implants due to their mechanical reliability, chemical stability, and biological compatibility. However, the bioinert nature of aluminum oxide makes it challenging for bone ingrowth and implant anchorage. To address this, ceramic scaffold samples with concentrated porosity have been developed. This study aimed to create porous Al_2O_3 and explore surface modifications using UV exposure, amino acid treatment (L-lysine), and alkaline treatment (NaOH) for applications in orthopedics and dentistry. The porous alumina samples underwent sintering at 1400°C and drying at 100°C . They were then analyzed for mechanical, morphological, and structural characteristics through various tests and microscopy techniques. The results revealed increased surface roughness after 16 hours of alkaline treatment and one hour of UV treatment, and decreased roughness with amino acid treatment for samples pre-treated with NaOH for 16 hours. Our results showed an increase in porosity with Alkaline and UV treatment and decrease with amino acid treatment, also results shows decrease in mechanical properties for alkali and UV treatments (Hardness and Compressive Strength) as it is in the range of cancellous bone strength. According to the current work, the contact angle between the untreated and treated samples with UV, amino acid, and NaOH was zero, which indicates that these surfaces are hyper hydrophilic. High porosity and surface roughness may be the cause of this behavior. Biological test evaluated by XRD and FESEM exhibited formation of Hydroxyapatite film when immersed in SBF for 7 days.

1. INTRODUCTION

Bio-inert ceramics are resistant to corrosion, sufficiently robust, biocompatible, and usually appealing (in the dental profession). However, its drawbacks, such as the absence of a direct bone-material interface, stress shielding, and the possibility for aseptic loosening, highlight the importance of surface changes [1]. With excellent strength, resistance to wear, and a smooth finish, alumina ceramics prove highly suitable as biomaterials [2-4]. They have created multiple items for the sockets or head of a hip joint prosthesis and are very helpful in orthopedic surgery for bone healing [2, 3]. Moreover, these ceramics are already in use in clinical settings for knee and ankle prosthesis components [3-5]. α -alumina is the most studied alumina phase [6], and it has recently been utilized in composite systems as a porous α -alumina base for bioactive materials [7]. The unique structure and composition of alumina substrates, coupled with their ability to attract cells and undergo chemical modifications that influence the growth of neural stem cells, make them excellent platforms for cell cultivation [8]. Studies have revealed that changing the chemical and surface properties of α -alumina can impact early

cell behavior, affecting how fibroblasts and cells similar to bone-forming osteoblasts grow, attach, and transform [9, 10]. To increase the surface area on ceramic materials, various techniques like oxidation, adding specific functional groups, silanization, heat treatments in controlled atmospheres, melt infiltration, or using ionizing liquid etching are employed, including processes like sol-gel methods and co-precipitation [11-15]. In dentistry, ceramics have been treated with mechanical techniques like sandblasting. However, sandblasting creates surface defects and residual stresses, which are significant drawbacks compared to chemical modification techniques. Fischer et al. [16] reported in 2005 that after a 24-hour soaking in a solution of 1 M NaOH at 100°C , hydroxyl (OH^-) functional groups had been effectively bound onto alumina substrates. When compared to the original, unmodified oxide of aluminum, it was shown that alkaline alteration of the adsorbent's surface improved the adsorption capacity [17]. A report by some researchers, an increase in aluminol, Al-OH, groups under specific conditions are achieved, these groups promote bioactivity and become nucleation centers for apatite growth also enhancing biointeraction with bone cells and can promote cell adhesion

to the artificial surface containing hydroxyl. As a result, aluminum hydroxide $[Al(OH)_4]^-$ may be a good choice for a bioactive substance [16], as these groups aid in the absorption of proteins and raise the material's wetness, which permits cell attachment and growth [18]. In order to manage the implant tissue interface, bio-functionalization enables the attachment of organic components on the implant surface, such as enzymes, proteins, and peptides [19]. L-arginine and L-lysine are two important amino acids that are involved in the formation and metabolism of bones [20, 21]. L-lysine is a renewable material that is found naturally [22]. L-lysine has been demonstrated to support osteogenic differentiation and proliferation of cells [23]. Patricia Comeau et al. in 2018 evaluated a three amino acids' affinity for the surface of non-stoichiometric hydroxyapatite nanoparticles. The degree of surface binding that was achieved actually seems to have been enhanced by the strong interaction that amine groups had with the negatively charged ns-nHA surface. Consequently, lysine and glycine bound to ns-nHA more firmly than aspartic acid at the reaction conditions that were investigated [24]. It has been reported that ultraviolet (UV) photo functionalization might enhance the conditions surrounding the implant abutment [25, 26]. Chairside application of the approach has multiple advantages, include a significant reduction in surface carbon concentration as well as enhanced wetting, proliferating, and adhesion of structure to cells [27, 28]. According to research conducted in 2022 by Rutkunas et al. [29], UV photo functionalization of Zirconia-based materials for abutment fabrication is a promising technique that may have an impact on the development of a strong peri-implant cover and support the integration of hard and soft tissue implants over the long term. They discovered that ZrO_2 -based materials photo functionalized on their UV surfaces change the survival of human gingival fibroblast cells, which may have positive effects on cell proliferation [29]. Henningsen et al. [30] assessed and contrasted the changes in the physicochemical surface conditions of zirconia surfaces following brief exposure to UV light. Zirconia samples with slightly rough surfaces underwent a 12-minute treatment in an ultraviolet (UV) oven, the tests revealed that the wetting ability zirconia surface was greatly enhanced by UV radiation. The goal of present study was to evaluate the effect of surface functionalization by NaOH solution, Lysine amino acid, and UV radiation on the mechanical, morphological and biological properties of alumina for bio applications. The advantages of these techniques are the creation of an active and rough surface that promotes adhesion and biologic fixation of implant and avoiding the drawback of other modification techniques like defects and residual stresses from sandblasting and creation of wear debris from coating.

2. EXPERIMENTAL PROCEDURES

2.1 Sample preparation

A cylinder compacted samples prepared using α - alumina powders (provided by Changsha Santech) with 99.9% purity and (1.3-12) μm particle size, that compressed by uniaxial pressure devices [(CT340-CT440)] green samples were dried at 100°C for 24 hours then sintered at 1400°C with heating rate (10°C/min) for 4 hours. Sintered samples were polished to get the smooth and perfect surface for treatments.

2.2 Surface treatments

2.2.1 Treatment by alkali solution

The samples were washed by deionized, then placed in a 5 M NaOH solution at 100°C for different times (12,16,20) hour. After that, samples were washed in deionized water and finally dried at 100°C. this process was done using the system in Figure 1.

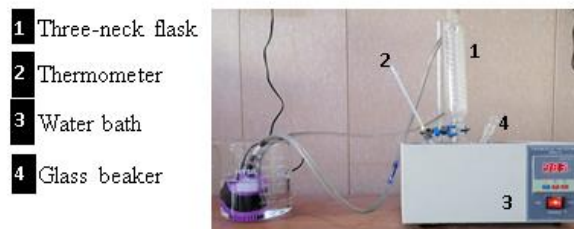


Figure 1. Working system

2.2.2 Amino acid treatment

The pre- treated samples with 5M NaOH solution for 16 hours were chosen as it has the highest roughness and surface area. Samples were soaked in a glass beaker with 50% w/v of Lysine (Provided by Transhuman Technologies) with 99.9 purity. for 24 hours at room temperature.

2.2.3 UV treatment

Pure alumina samples were exposed to UV radiation with wave length 254 nm for one hour using (NASWIETLACZ UV 254-8), as shown in Table 1.

Table 1. Explaining specimens symbols according to the surface treatments

Ao	Pure Specimens before Treatment
A ₁₂	Specimen treated with 5M NaOH for 12 hours at 100°C
A ₁₆	Specimen treated with 5M NaOH for 16 hours at 100°C
L ₁₆	Pre-treated specimen with 5M NaOH for 16 hours than 50W/V% amino acid (Lysine) 24 hours
U ₁	Specimen treated with ultraviolet waves for 1 hour

3. CHARACTERIZATION

3.1 X-ray diffractometer

X-ray diffractometer device (XRD 6000, Shimadzo, Japan) with Cu $k\alpha$ radiation ($\lambda=1.5405 \text{ \AA}$), and 5°/min scanning speed was used to characterize the phase composition and fixing the structural properties of samples.

3.2 Fourier Transforms Infrared Spectrometer (FTIR)

The functional groups (OH, NH, COOH, CH) present on the surface before and after treatment was recognized by FTIR (Fourier Transform Infrared Spectrophotometer, SHIMADZU 1800, Japan). The wavenumber was in the middle of the range (500-4000 cm^{-1}).

3.3 Roughness assessment

The roughness of the surfaces in the samples was measured using AFM (Atomic Force Microscopy) before and after

treatment to observe how the treatment impacted the surface area. The AFM concept relies on the mechanical interaction between the surface and the tip. The AFM (AA3000) tapping mode was employed for the analysis. The findings were illustrated using surface roughness, specifically the average roughness (Ra).

3.4 Field emission Scanning Electron Microscopy (FESEM)

Surface morphology of all Sample groups was described by (FESEM-Imaging-EDX-Mapping-Line-EBSD/Germany) using Field emission Scanning Electron Microscopy (FESEM) after coating with a thin layer of gold.

3.5 Physical and mechanical properties

The Archimedes method was employed to determine the density and apparent porosity of alumina sample both before and after treatment, according to with ASTM C20. Using the following equations

$$\text{Density is equal to } WD/(Ws - WI) \quad (1)$$

$$\text{Appearance Porosity} = (Ws - WD/WS - WI) \times 100 \quad (2)$$

where, *WD* is weight of the dry scaffold; *WS* is weight of the soaked scaffold; and *WI* is weight of the immersed scaffold.

Maximum compressive strength were estimated for samples before and after treatments by (Model(DSCK)). A mechanical tester with 0.2 mm/sec crosshead speed was used; three samples at least, were tested to get the average strength value.

Vickers Micro-hardness of specimens was examined using an HVS-1000, Laryee, Digital Micro-hardness tester with a force of 4.9N and a holding duration of 15 seconds. three samples, at least, were tested to get the average hardness value, which was carried out in accordance with ASTM E3841. using the following equation:

$$Hv = 1.854(p/d^2) \quad (3)$$

where, *Hv* is the Vickers hardness (Mpa); *p* is load (N); *D* is diagonal length of the indentation impression (μm). For all physical and mechanical tests; three samples, at least, were used to get the average value.

3.6 Bioactivity evaluation

In order to evaluate the bioactivity of treated samples, they immersed in SBF at 37°C for 7 days. FESEM was used and XRD analysis was carried out for the surfaces at the end of immersion time to check hydroxyapatite formation.

4. RESULT AND DISCUSSION

4.1 X-ray diffraction

4.1.1 Alkaline treatment

Figure 2 shows XRD patterns for alumina samples treated with NaOH solution at different time. It can be noted the appearance of AL(OH)₃, and ALO(OH) peaks for A₁₂ that approved with standard cards number (JCPDS No.01-089-4333) and, (01-070-2138) respectively. While the surface of

A₁₆ and A₂₀ samples exhibit the AL(OH)₃ according to (JCPDS) card No. (00-018-0031) and (00-026-0025) respectively. the characteristic peaks of Al₂O₃ appeared according to (JCPDS) card No. 01-089-3072). These results proved an increasing hydroxyl group on the surface with increasing the treatment time [31-33]. Gibbsite's layered structure's volatilization of water most likely initiated the phase shift from gibbsite to boehmite [34]. The following procedure converted the aluminum dioxide that was exposed at the outer layer to aluminum hydroxide [16]:

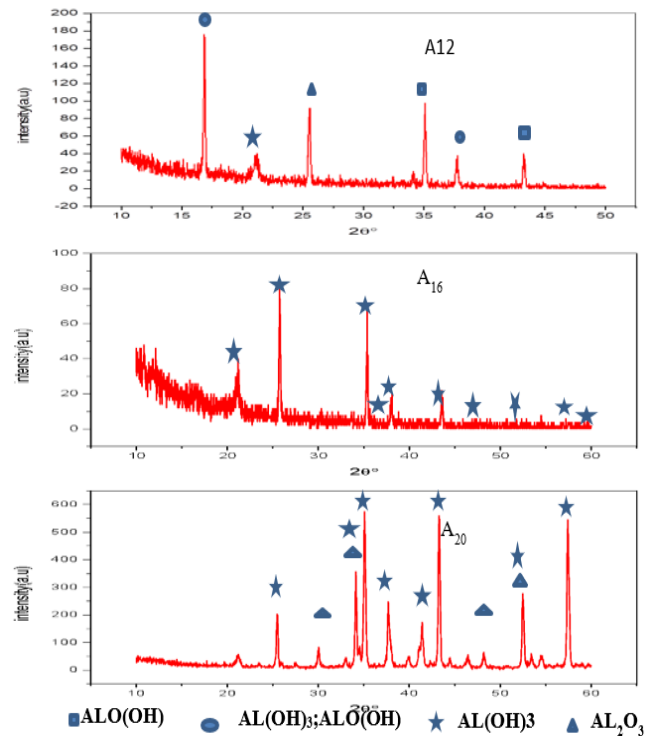


Figure 2. XRD pattern for alkali treated samples (A₁₂, A₁₆, A₂₀)

4.1.2 Acid treatment, UV treatment

Figure 3 displays X-ray diffraction (XRD) patterns of the (L₁₆) Alumina sample treated with lysine at a 50% weight/volume ratio for 24 hours. The pattern confirms the presence of C₆H₁₄N₂O₂, matching the standard card number (JCPDS No.00-021-1717) [35, 36]. Additionally, characteristic peaks of Al₂O₃ are identified based on the standard card number (JCPDS No. JCPDS: 00-046-1212). Furthermore, Figure 3 illustrates the XRD pattern of the (U1) Alumina samples treated with ultraviolet (UV) light for one hour, indicating the existence of AL(OH)₃ in accordance with the standard card number (JCPDS No. 01-085-1049).

4.2 Fourier TRANSFORMS Infrared Spectrometer (FTIR)

Figure 4 reveals FTIR spectra for samples treated with NaOH solution in different time. For all samples the functional group (OH⁻) are characteristic band of absorbed water (at the range 3417.86-3471.87 cm⁻¹ at different intensities. Broad peak occurs at 3424 cm⁻¹ is related to the OH⁻ groups that are adsorbed on the surface [32]. The band at 455cm⁻¹, 462cm⁻¹, 601cm⁻¹ in A₁₂, A₁₆, A₂₀ respectively is assigned for the stretching modes of (Al-O) bond. In general Figure 4

confirmed that with increasing the treatment time the broad band related to OH⁻ vibration increased in intensity. The results of this treatment confirmed by Niedhart et al. [37], who treated alumina ceramic surface by sodium hydroxide solution to produce biologically active OH⁻ groups.

Figure 5 shows FTIR spectra for samples treated with amino acid (L₁₆). The bands at the range 447.94-678.94 cm⁻¹ are assigned to the Al-O. while the bands at the range 2816.07-3425.58 cm⁻¹ are assigned to the CH₂, OH. we notice a decrease in the OH group at different intensities L₁₆. the range at 1427.32-1581.63cm⁻¹ related peaks to COOH [38, 39]. Based on results, a chemical reaction between superficial hydroxyl groups of the alumina Sample and the amino acids molecules, causing the formation of amino acids as coupling agents on the surface of Sample [38]. Also Figure 5 appear FTIR spectra for samples treated with UV (U₁). The bands at the range 462.92-655.80 cm⁻¹ are assigned to the Al-O. The broad absorption peak at range 3417.86-3479.58 cm⁻¹ at different intensities attributed to OH⁻ group [39].

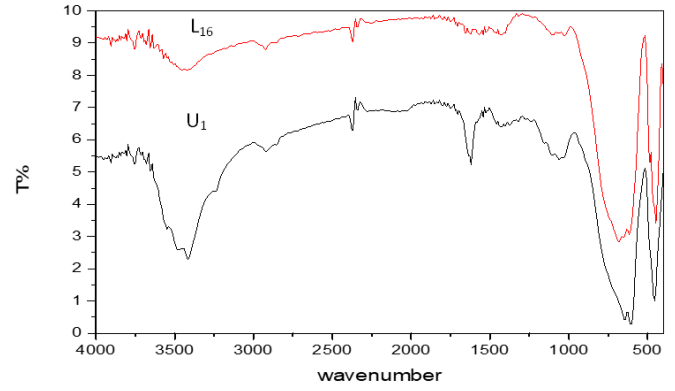


Figure 5. FTIR spectra for alumina samples treated with: Amino acid (L₁₆), Ultraviolet radiation (U₁)

4.3 Roughness results

Figure 6 shows the variation of surface roughness for alumina samples after different treatments. It is worth pointing out that high roughness belongs to UV treatment as confirmed by FESEM images. Table 2 summarizes the surface roughness and surface area for samples groups. The results demonstrate that increasing treatment time in NaOH, leading to rise of roughness and surface area these results confirmed by other researches [40]. While roughness decreases after amino acid (Lysine) treatment, this result achieved to formation of thin layer of amino acid molecules as confirmed by XRD results in Figure 3. The capacity to change the surface characteristics of porous α -alumina to generate the ideal biocompatible and bioactive material is demonstrated by all of the above outcomes. It was discovered that the adhesion, proliferating, and differentiating of living osteoblast-like cells were significantly impacted by the surface rough of an alumina-based scaffold [41].

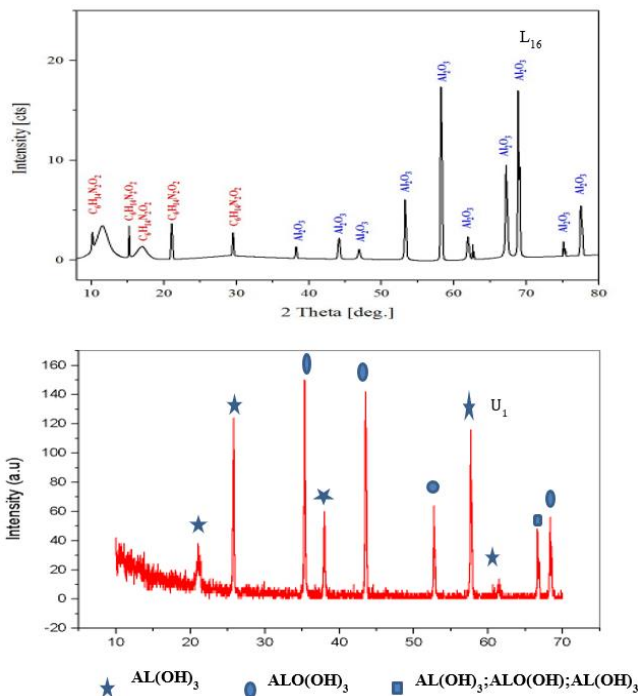


Figure 3. XRD pattern for alumina samples treated with: Amino acid (L₁₆), Ultraviolet radiation (U₁)

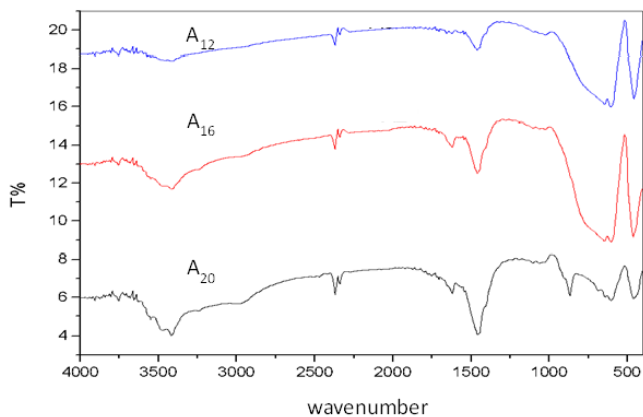


Figure 4. FTIR spectra for alkali treated samples (A₁₂, A₁₆, A₂₀)

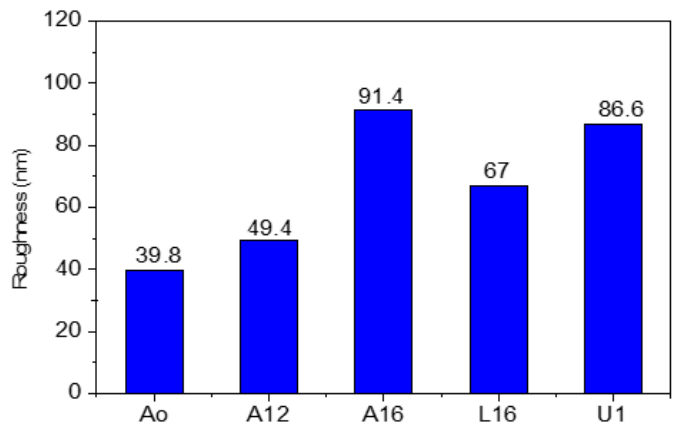


Figure 6. Surface roughness for alumina samples treated with different condition

Table 2. Surface roughness for alumina samples treated with different condition

Sample	Roughness Average	Surface Area Ratio
Ao	39.8	4.649
A12	49.4	9.35
A16	91.4	17.5
L16	67	10.6
U1	86.8	16.74

4.4 Microstructure characterization

In Figure 7, we can observe the surface topography of alumina samples subjected to various treatments. The images obtained from FESEM validate the findings on the materials' physical and mechanical characteristics. Treating the samples with a sodium hydroxide solution resulted in a porous and

rough surface. According to Abegunde et al. [40], the specific surface area and pore volume concentration increased as the concentration of the alkali solution rose. On the other hand, the L₁₆ image displays lower porosity and smaller pore sizes. Conversely, UV treatment led to a surface with clearly visible pore sizes.

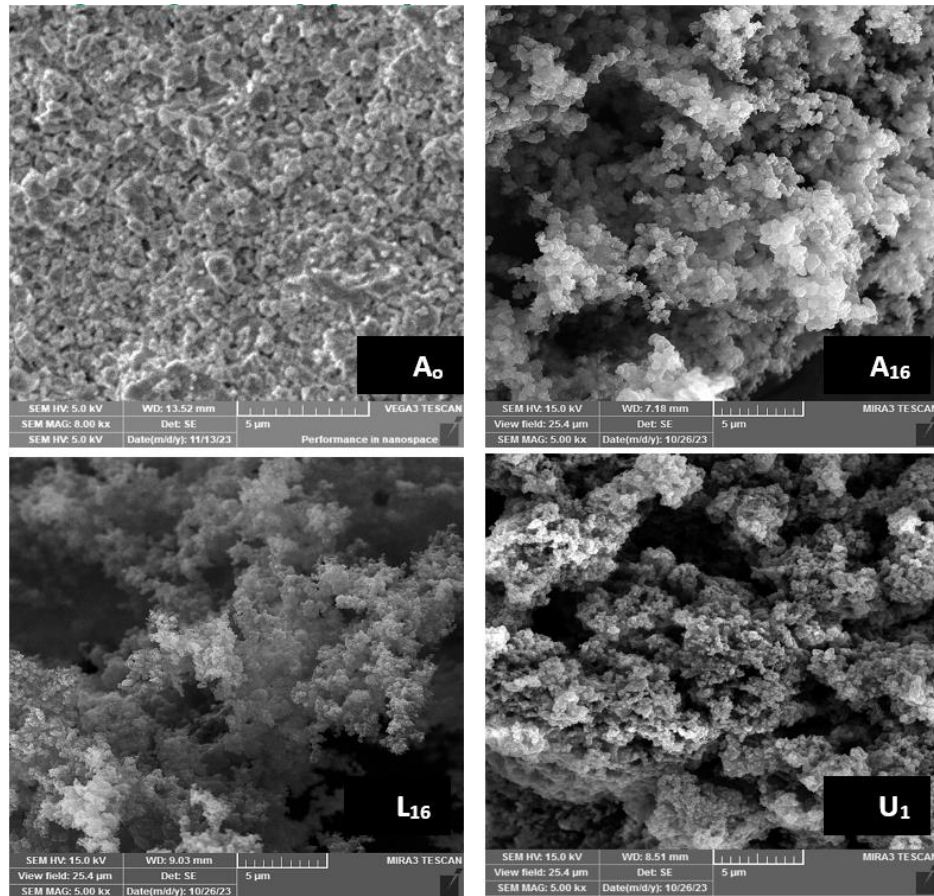


Figure 7. FESEM of sample treated with different conditions (A₁₆, L₁₆, U₁), A₀:pure sample

4.5 Physical and mechanical results

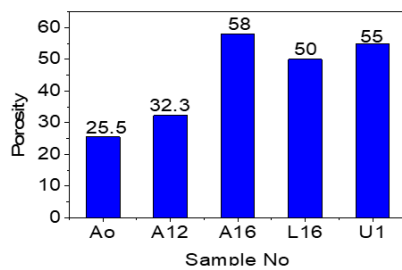


Figure 8. Alumina porosity before and after different treatments

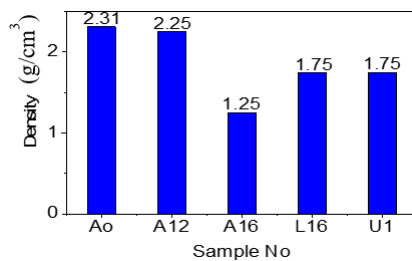


Figure 9. Alumina density before and after different treatments

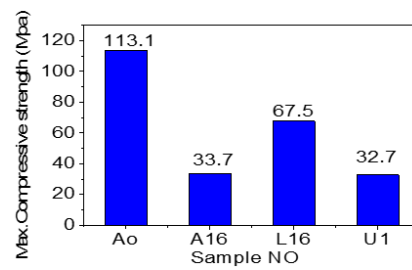


Figure 10. Alumina strength before and after different treatments

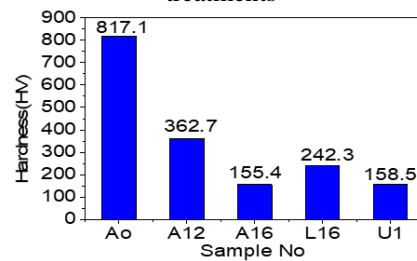


Figure 11. Alumina hardness before and after different treatments

Figure 8 clearly shows that all surface treatments increase the porosity of the original alumina (Ao) and result in a decrease in density, as depicted in Figure 9. These findings are confirmed by FESEM images. A study revealed that a selective chemical etching of zirconia toughened alumina surfaces led to a nano-rough and interconnected porous surface [8]. A₁₆, L₁₆, and U₁ exhibit acceptable porosity to serve as a scaffold for bone tissue engineering, as confirmed by Costa et al. [42] who developed micro-macroporous alpha-alumina scaffolds with high potential for use in bone tissue engineering.

The physical property results indicate a reduction in hardness and compressive strength, as illustrated in Figure 10 and Figure 11. The original alumina sample demonstrates the highest mechanical properties, while treatment with a 5M NaOH alkali solution for 16 hours, as well as UV treatment, led to a significant decrease in compressive strength due to surface attack and roughening. There is also a less pronounced decrease in compressive strength for alumina samples treated with amino acid, resulting from the creation of a thin layer covering the small pores and filling micro cracks on the surfaces, inducing a crack bridging mechanism [43, 44]. This causes an increase in the compressive resistance of L₁₆ compared with A₁₆ and U₁.

Table 3 shows that the compressive strength of the porous alumina sample before surface treatment falls within the range of 90-209 MPa, which is comparable to the strength of human cortical bone. This indicates that it is well-suited for applications that require bearing heavy loads. However, after undergoing surface treatment, the compressive strength of the treated samples falls within the range of 1.5-45 MPa, which is similar to cancellous bone [45].

Table 3. Summarized some physical and mechanical properties of alumina samples treated with different conditions

Sample	Density (g/cm ³)	Porosity%	Hardness (HV)	Compressive Strength (MPa)
Ao	2.315	25.5	817.1	113.1
A ₁₂	2.25	32.2	362.7
A ₁₆	1.25	58	155.4	33.7
L ₁₆	1.75	50	289.9	67.5
U ₁	1.75	55	158.5	32.7

4.6 Biological results

4.6.1 Bioactivity evaluation

In Figure 12 All XRD profiles confirm the formation of hydroxyapatite (HA) phase. (AL₂O₃) peaks were present for all samples with different intensity approving with standard cards number (JCPDS No.00-046-1212) which indicate the substrate material. Also, the figure demonstrates the existence of Ca₁₀(PO₄)₆(OH)₂ phase that approving with standard cards number (JCPDS No.01-072-1243) for A₁₆ and (JCPDS No. 01-086-0740) for L₁₆. It has been found that for the hydroxylated surfaces, certain conditions lead to a rise in aluminol, or Al-OH, groups, which then serve as nucleation nuclei for the formation of apatite [16]. A surface that is strongly hydroxylated enhances the capacity of α-alumina to absorb calcium ions and initiates the nucleation of calcium phosphate, resulting to the formation of apatite on alumina in vitro. Additionally, the XRD pattern for (U₁) demonstrates the presence of a typical card number (JCPDS No. 00-010-0348), which is the Ca approval.

4.6.2 FESEM images

Figure 13 shows FESEM images for alumina samples treated with different conditions after immersed in SBF for 7 days. Obvious changes were noticed on all surfaces indicate to the formation of a hydroxyapatite agglomeration which confirmed by XRD results. As reported by Mozafari et al. [46], alumina ceramic that had been treated with NaOH had better apatite nucleation than untreated alumina surface. On etched samples, a thin, granular in nature nano-porous layer of apatite nucleated, approximately covering all of the surface. The etched samples are thought to have created a thin film of sodium β-alumina, which is resistant to being removed through washing due to their nano-rough surface. The same indication presents on the image of L₁₆. This agrees with the finding of Tavafoghi and Cerruti [47] who mentioned that amino acids bound to surfaces promote HA precipitation by attracting Ca²⁺ and PO₄³⁻ ions and increasing the local supersaturation, that could introduce to new research filed for bone regeneration as a therapeutic manner. Matsumoto et al. [48] found flake-like particles consisting of nano-sized platelets for HA precipitation in the presence of Amino acids. The flake-like HA morphology was also reported by Eiden-Aßmann et al. [49] who found that presence of charged Amino Acids, such as Glu, Asp, arginine (Arg) and lysine (Lys), show a significantly stronger effect than non-charged ones. Similar hydroxyapatite agglomeration had been shown on the surface of U₁ sample indicating that UV-irradiated AL₂O₃ possess good apatite-forming ability which supported by the results of Lee et al. [50, 51] who found that UV light treatment could effectively induce bone-like apatite formation in a short time in SBF as it play a crucial role in producing OH groups on the surface of oxide layer helped to induce the growth of bone-like apatite by providing more nucleation sites. Also, Yeo [52] reported that the stability of implants inserted into the patients' jaw bones increased more rapidly when the implants were UV-photo functionalized.

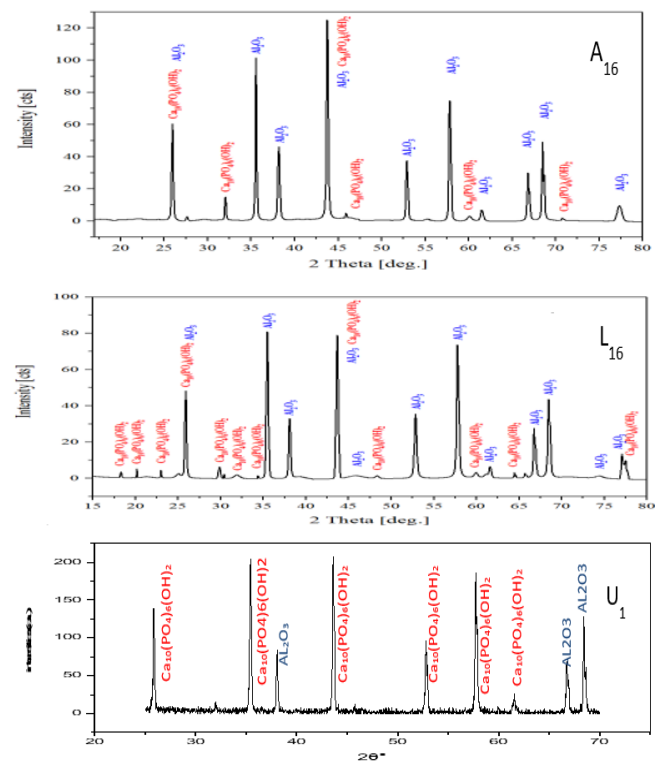


Figure 12. XRD analysis for treated alumina samples after immersed in SBF for 7 days

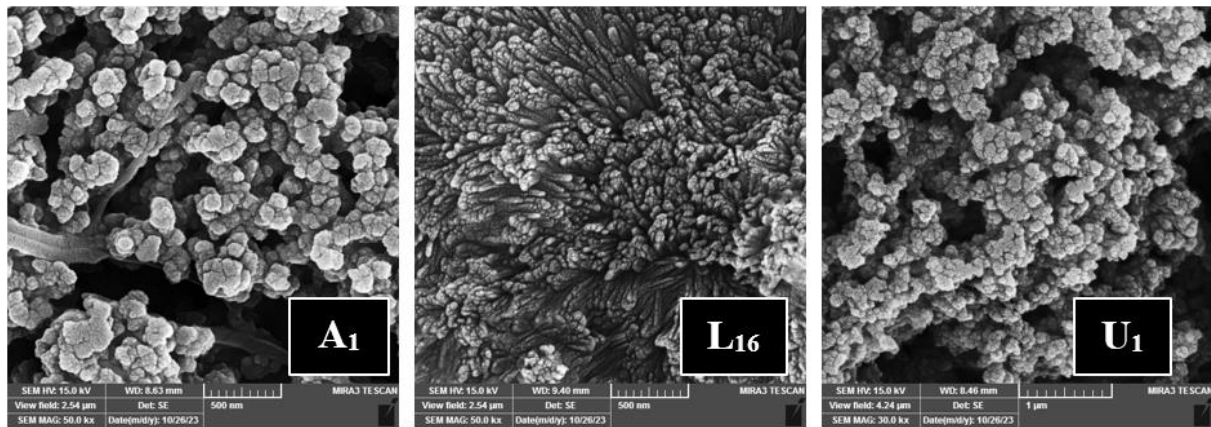


Figure 13. FESEM images for alumina samples treated with different conditions after immersed in SBF for 7 days

5. CONCLUSION

The use of alumina in prosthetic hip and knee joints has the advantage of significantly reducing bearing wear rates porous alumina has attracted a lot of interest for usage as scaffolds, especially when it comes to cell loading and bone grafting. Different surface modification techniques were successfully used to modify alumina surface for bioapplications it was found that alumina treated by alkali solution (5 M NaOH), amino acid (lysine) and ultraviolet radiation showed presence of hydroxyl group on the surface with increasing porosity and surface roughness leading to a reduction in compressive strength. According to these finding, treated alumina samples could introduce as scaffold for bone tissue engineering in non-load bearing sites. Because all treated samples showed bioactivity behavior via forming agglomeration of HA in vitro. it was found that by controlling the formation of functional groups on alumina surface, the physical, chemical and biological properties of implant could be changed to create a successful implant with acceptable roughness for direct fixation and promote tissue ingrowth. The higher wettability of samples has been associated to great lubrication introducing it as good candidate for joints prosthetic. Finally it is important to recommend for cell culture test to evaluate cell response towards treated surfaces, also estimating wear rate for modified surfaces will provide an evaluation for using them in joint prosthetic.

REFERENCES

- [1] Stanciuc, A.M. (2017). In vitro evaluation of cell-material interactions on bioinert ceramics with novel surface modifications for enhanced osseointegration. Doctoral dissertation, Université de Lyon.
- [2] Boutin, P., Christel, P., Dorlot, J.M., Meunier, A., De Roquancourt, A., Blanquaert, D., Witvoet, J. (1988). The use of dense alumina-alumina ceramic combination in total hip replacement. *Journal of Biomedical Materials Research*, 22(12): 1203-1232. <https://doi.org/10.1002/jbm.820221210>
- [3] Lee, Y.K., Ha, Y.C., Yoo, J.J., Koo, K.H., Yoon, K.S., & Kim, H.J. (2010). Alumina-on-alumina total hip arthroplasty: A concise follow-up, at a minimum of ten years, of a previous report. *The Journal of Bone & Joint Surgery*, 92(8): 1715-1719. <https://doi.org/10.2106/JBJS.I.01019>
- [4] Bal, B.S., Greenberg, D.D., Buhrmester, L., Aleto, T.J. (2006). Primary TKA with a zirconia ceramic femoral component. *The Journal of Knee Surgery*, 19(2): 89-93. <https://doi.org/10.1055/s-0030-1248085>
- [5] Ohgushi, H., Kotobuki, N., Funaoka, H., Machida, H., Hirose, M., Tanaka, Y., Takakura, Y. (2005). Tissue engineered ceramic artificial joint-ex vivo osteogenic differentiation of patient mesenchymal cells on total ankle joints for treatment of osteoarthritis. *Biomaterials*, 26(22): 4654-4661. <https://doi.org/10.1016/j.biomaterials.2004.11.055>
- [6] Mavrič, A., Valant, M., Cui, C., Wang, Z.M. (2019). Advanced applications of amorphous alumina: From nano to bulk. *Journal of Non-Crystalline Solids*, 521: 119493. <https://doi.org/10.1016/j.jnoncrysol.2019.119493>
- [7] Urbonavicius, M., Varnagiris, S., Pranevicius, L., Milcius, D. (2020). Production of gamma alumina using plasma-treated aluminum and water reaction byproducts. *Materials*, 13(6): 1300. <https://doi.org/10.3390/ma13061300>
- [8] Kühn, P.T. (2016). The effect of wettability and stiffness on stem cell behavior at bioinert surfaces. Doctor of Philosophy, University of Groningen.
- [9] Wittenbrink, I., Hausmann, A., Schickle, K., Lauria, I., Davtalab, R., Foss, M., Fischer, H. (2015). Low-aspect ratio nanopatterns on bioinert alumina influence the response and morphology of osteoblast-like cells. *Biomaterials*, 62: 58-65. <https://doi.org/10.1016/j.biomaterials.2015.05.026>
- [10] Duraccio, D., Strongone, V., Faga, M.G., Auriemma, F., Mussano, F.D., Genova, T., Malucelli, G. (2019). The role of different dry-mixing techniques on the mechanical and biological behavior of UHMWPE/alumina-zirconia composites for biomedical applications. *European Polymer Journal*, 120: 109274. <https://doi.org/10.1016/j.eurpolymj.2019.109274>
- [11] Yan, M., Csik, A., Yang, C.C., Luo, Y., Fodor, T., Ding, S.J. (2018). Synergistic reinforcement of surface modification on improving the bonding of veneering ceramics to zirconia. *Ceramics International*, 44(16): 19665-19671. <https://doi.org/10.1016/j.ceramint.2018.07.218>
- [12] Ilyas, A., Muhammad, N., Gilani, M.A., Vankelecom, I.F., Khan, A.L. (2018). Effect of zeolite surface

- modification with ionic liquid [APTMS][Ac] on gas separation performance of mixed matrix membranes. *Separation and Purification Technology*, 205: 176-183. <https://doi.org/10.1016/j.seppur.2018.05.040>
- [13] Cremers, V., Rampelberg, G., Barhoum, A., Walters, P., Claes, N., de Oliveira, T.M., Detavernier, C. (2018). Oxidation barrier of Cu and Fe powder by atomic layer deposition. *Surface and Coatings Technology*, 349: 1032-1041. <https://doi.org/10.1016/j.surfcoat.2018.06.048>
- [14] Rao, P.K., Jana, P., Ahmad, M.I., Roy, P.K. (2019). Synthesis and characterization of zirconia toughened alumina ceramics prepared by co-precipitation method. *Ceramics International*, 45(13): 16054-16061, <https://doi.org/10.1016/j.ceramint.2019.05.121>
- [15] Monteiro, J.B., Oliani, M.G., Guilardi, L.F., Prochnow, C., Pereira, G.K.R., Bottino, M.A., Valandro, L.F. (2018). Fatigue failure load of zirconia-reinforced lithium silicate glass ceramic cemented to a dentin analogue: Effect of etching time and hydrofluoric acid concentration. *Journal of the Mechanical Behavior of Biomedical Materials*, 77: 375-382. <https://doi.org/10.1016/j.jmbbm.2017.09.028>
- [16] Fischer, H., Niedhart, C., Kaltenborn, N., Prange, A., Marx, R., Niethard, F.U., Telle, R. (2005). Bioactivation of inert alumina ceramics by hydroxylation. *Biomaterials*, 26(31): 6151-6157. <https://doi.org/10.1016/j.biomaterials.2005.04.038>
- [17] Reshetnikov, S., Kurzina, I., Livanova, A., Meshcheryakov, E., Isupova, L. (2019). Effect of Li, Na and K modification of alumina on its physical and chemical properties and water adsorption ability. *Materials*, 12(24): 4212. <https://doi.org/10.3390/ma12244212>
- [18] Morterra, C., Magnacca, G. (1996). A case study: Surface chemistry and surface structure of catalytic aluminas, as studied by vibrational spectroscopy of adsorbed species. *Catalysis Today*, 27(3-4): 497-532, [https://doi.org/10.1016/0920-5861\(95\)00163-8](https://doi.org/10.1016/0920-5861(95)00163-8)
- [19] Morra, M. (2006). Biochemical modification of titanium surfaces: peptides and ECM proteins. *Eur Cell Mater*, 12(1): 15, <https://doi.org/10.22203/eCM.v012a01>
- [20] Fini, M., Torricelli, P., Giavaresi, G., Carpi, A., Nicolini, A., Giardino, R. (2001). Effect of L-lysine and L-arginine on primary osteoblast cultures from normal and osteopenic rats. *Biomedicine & pharmacotherapy*, 55(4): 213-220. [https://doi.org/10.1016/S0753-3322\(01\)00054-3](https://doi.org/10.1016/S0753-3322(01)00054-3)
- [21] Torricelli, P., Fini, M., Giavaresi, G., Giardino, R., Gnudi, S., Nicolini, A., Carpi, A. (2002). L-arginine and L-lysine stimulation on cultured human osteoblasts. *Biomedicine & Pharmacotherapy*, 56(10): 492-497. [https://doi.org/10.1016/S0753-3322\(02\)00287-1](https://doi.org/10.1016/S0753-3322(02)00287-1)
- [22] Chen, X., Lai, H., Xiao, C., Tian, H., Chen, X., Tao, Y., Wang, X. (2014). New bio-renewable polyester with rich side amino groups from L-lysine via controlled ring-opening polymerization. *Polymer Chemistry*, 5(22): 6495-6502. <https://doi.org/10.1039/C4PY00930D>
- [23] Zheng, S., Guan, Y., Yu, H., Huang, G., Zheng, C. (2019). Poly-L-lysine-coated PLGA/poly (amino acid)-modified hydroxyapatite porous scaffolds as efficient tissue engineering scaffolds for cell adhesion, proliferation, and differentiation. *New Journal of Chemistry*, 43(25): 9989-10002. <https://doi.org/10.1039/C9NJ01675A>
- [24] Comeau, P., Willett, T. (2018). Impact of side chain polarity on non-stoichiometric nano-hydroxyapatite surface functionalization with amino acids. *Scientific Reports*, 8(1): 12700. <https://doi.org/10.1038/s41598-018-31058-5>
- [25] Guo, L., Smeets, R., Kluwe, L., Hartjen, P., Barbeck, M., Cacaci, C., Henningsen, A. (2019). Cytocompatibility of titanium, zirconia and modified PEEK after surface treatment using UV light or non-thermal plasma. *International Journal of Molecular Sciences*, 20(22): 5596. <https://doi.org/10.3390/ijms20225596>
- [26] Yang, Y., Zhou, J., Liu, X., Zheng, M., Yang, J., Tan, J. (2015). Ultraviolet light-treated zirconia with different roughness affects function of human gingival fibroblasts in vitro: The potential surface modification developed from implant to abutment. *Journal of Biomedical Materials Research Part B: Applied Biomaterials*, 103(1): 116-124. <https://doi.org/10.1002/jbm.b.33183>
- [27] Tuna, T., Wein, M., Swain, M., Fischer, J., Att, W. (2015). Influence of ultraviolet photofunctionalization on the surface characteristics of zirconia-based dental implant materials. *Dental Materials*, 31(2): e14-e24. <https://doi.org/10.1016/j.dental.2014.10.008>
- [28] Yang, Y., Zheng, M., Liao, Y., Zhou, J., Li, H., Tan, J. (2019). Different behavior of human gingival fibroblasts on surface modified zirconia: A comparison between ultraviolet (UV) light and plasma. *Dental Materials Journal*, 38(5): 756-763. <https://doi.org/10.4012/dmj.2018-101>
- [29] Rutkunas, V., Borusevicius, R., Balciunas, E., Jasinskyte, U., Alksne, M., Simoliunas, E., Mijiritsky, E. (2022). The effect of UV treatment on surface contact angle, fibroblast cytotoxicity, and proliferation with two types of zirconia-based ceramics. *International Journal of Environmental Research and Public Health*, 19(17): 11113. <https://doi.org/10.3390/ijerph191711113>
- [30] Henningsen, A., Smeets, R., Heuberger, R., Jung, O.T., Hanken, H., Heiland, M., Precht, C. (2018). Changes in surface characteristics of titanium and zirconia after surface treatment with ultraviolet light or non-thermal plasma. *European Journal of Oral Sciences*, 126(2): 126-134. <https://doi.org/10.1111/eos.12400>
- [31] Souza, A.D., Arruda, C.C., Fernandes, L., Antunes, M.L., Kiyohara, P.K., Salomão, R. (2015). Characterization of aluminum hydroxide (Al (OH) 3) for use as a porogenic agent in castable ceramics. *Journal of the European Ceramic Society*, 35(2): 803-812. <https://doi.org/10.1016/j.jeurceramsoc.2014.09.010>
- [32] Goudarzi, M., Ghanbari, D., Salavati-Niasari, M., Ahmadi, A. (2016). Synthesis and characterization of Al(OH)₃, Al₂O₃ nanoparticles and polymeric nanocomposites. *Journal of Cluster Science*, 27: 25-38.
- [33] Faga, M.G., Vallée, A., Bellosi, A., Mazzocchi, M., Thinh, N.N., Martra, G., Coluccia, S. (2012). Chemical treatment on alumina-zirconia composites inducing apatite formation with maintained mechanical properties. *Journal of the European Ceramic Society*, 32(10): 2113-2120. <https://doi.org/10.1016/j.jeurceramsoc.2011.12.020>
- [34] Vasile, B.S., Dobra, G., Iliev, S., Cotet, L., Neacsu, I.A., Nicoara, A.I., Filipescu, L. (2021). Thermally activated Al (OH)3: Part I—morphology and porosity evaluation. *Ceramics*, 4(2): 265-277. <https://doi.org/10.3390/ceramics4020021>

- [35] Ngouoko, J.J.K., Tajeu, K.Y., Temgoua, R.C.T., Doungmo, G., Doench, I., Tamo, A.K., Tonle, I.K. (2022). Hydroxyapatite/L-lysine composite coating as glassy carbon electrode modifier for the analysis and detection of Nile blue A. *Materials*, 15(12): 4262. <https://doi.org/10.3390/ma15124262>
- [36] Kambara, O., Tamura, A., Uchino, T., Yamamoto, K., Tominaga, K. (2010). Terahertz time-domain spectroscopy of poly-L-lysine. *Biopolymers: Original Research on Biomolecules*, 93(8): 735-739. <https://doi.org/10.1002/bip.21467>
- [37] Niedhart, C., Sax, M., Geschwill, K., Telle, R., Niethard, F.U. (2003). Enhancement of in vitro Bioactivity resulting from the Hydroxylation of Oxide Ceramic Surfaces. In *Bioceramics in Joint Arthroplasty: 8 th BIOLOX® Symposium Berlin*, pp. 111-117.
- [38] Fereshteh, Z., Mallakpour, F., Fathi, M., Mallakpour, S., Bagri, A. (2015). Surface modification of Mg-doped fluoridated hydroxyapatite nanoparticles using bioactive amino acids as the coupling agent for biomedical applications. *Ceramics International*, 41(8): 10079-10086. <https://doi.org/10.1016/j.ceramint.2015.04.101>
- [39] Berthomieu, C., Hienerwadel, R. (2009). Fourier transform infrared (FTIR) spectroscopy. *Photosynthesis Research*, 101: 157-170.
- [40] Abegunde, S.M., Idowu, K.S., Adejuwon, O.M., Adeyemi-Adejolu, T. (2020). A review on the influence of chemical modification on the performance of adsorbents. *Resources, Environment and Sustainability*, 1: 100001. <https://doi.org/10.1016/j.resenv.2020.100001>
- [41] Silva, J.R.S., Santos, L.N.R.M., Farias, R.M.C., Sousa, B.V., Neves, G.A., Menezes, R.R. (2022). Alumina applied in bone regeneration: Porous α -alumina and transition alumina. *Cerâmica*, 68: 355-363. <https://doi.org/10.1590/0366-69132022683873335>
- [42] Costa, H.D.S., Pereira, M.M., Andrade, G.I., Stancioli, E.F.B., Mansur, H.S. (2007). Characterization of calcium phosphate coating and zinc incorporation on the porous alumina scaffolds. *Materials Research*, 10: 27-29. <https://doi.org/10.1590/S1516-14392007000100007>
- [43] Deng, Z.Y., Fukasawa, T., Ando, M., Zhang, G.J., Ohji, T. (2001). Microstructure and mechanical properties of porous alumina ceramics fabricated by the decomposition of aluminum hydroxide. *Journal of the American Ceramic Society*, 84(11): 2638-2644. <https://doi.org/10.1111/j.1151-2916.2001.tb01065.x>
- [44] Philippart, A., Boccaccini, A.R., Fleck, C., Schubert, D. W., Roether, J.A. (2015). Toughening and functionalization of bioactive ceramic and glass bone scaffolds by biopolymer coatings and infiltration: A review of the last 5 years. *Expert Review of Medical Devices*, 12(1): 93-111. <https://doi.org/10.1586/17434440.2015.958075>
- [45] Ginebra, M.P., Espanol, M., Maazouz, Y., Bergez, V., Pastorino, D. (2018). Bioceramics and bone healing. *EFORT Open Reviews*, 3(5): 173-183. <https://doi.org/10.1302/2058-5241.3.170056>
- [46] Mozafari, M., Rabiee, M., Azami, M., Maleknia, S. (2010). Biomimetic formation of apatite on the surface of porous gelatin/bioactive glass nanocomposite scaffolds. *Applied Surface Science*, 257(5): 1740-1749. <https://doi.org/10.1016/j.apsusc.2010.09.008>
- [47] Tavafoghi, M., Cerruti, M. (2016). The role of amino acids in hydroxyapatite mineralization. *Journal of The Royal Society Interface*, 13(123): 20160462. <https://doi.org/10.1098/rsif.2016.0462>
- [48] Matsumoto, T., Okazaki, M., Inoue, M., Hamada, Y., Taira, M., Takahashi, J. (2002). Crystallinity and solubility characteristics of hydroxyapatite adsorbed amino acid. *Biomaterials*, 23: 2241-2247. [https://doi.org/10.1016/S0142-9612\(01\)00358-1](https://doi.org/10.1016/S0142-9612(01)00358-1)
- [49] Eiden-Aßmann, S., Viertelhaus, M., Heiß, A., Hoetzer, K.A., Felsche, J. (2002). The influence of amino acids on the biomineralization of hydroxyapatite in gelatin. *Journal of Inorganic Biochemistry*, 91(3): 481-486. [https://doi.org/10.1016/S0162-0134\(02\)00481-6](https://doi.org/10.1016/S0162-0134(02)00481-6)
- [50] Lee, T.C., Idris, M.I., Abdullah, H.Z. (2015). Effect of UV light treatment condition on apatite formation of anodised titanium. *Advanced Materials Research*, 1125: 460-464. <https://doi.org/10.4028/www.scientific.net/AMR.1125.460>
- [51] Lee, T.C., Abdullah, H.Z., Koshy, P., Idris, M.I. (2018). Ultraviolet-assisted biomimetic coating of bone-like apatite on anodised titanium for biomedical applications. *Thin Solid Films*, 660: 191-198. <https://doi.org/10.1016/j.tsf.2018.06.021>
- [52] Yeo, I.S.L. (2019). Modifications of dental implant surfaces at the micro-and nano-level for enhanced osseointegration. *Materials*, 13(1): 89. <https://doi.org/10.3390/ma13010s089>